Author Manuscript

Author Manuscript

Author Manuscript

Author Manuscript

HHS Public Access

Author manuscript

J Oral Maxillofac Surg Med Pathol. Author manuscript; available in PMC 2016 March 01.

Published in final edited form as:

J Oral Maxillofac Surg Med Pathol. 2015 March ; 27(2): 159–165. doi:10.1016/j.ajoms.2013.12.003.

Image-guided Interstitial Photodynamic Therapy for Squamous Cell Carcinomas: Preclinical investigation

Mirabelle Sajisevi[a], **Nestor R Rigual**[a,b], **David A. Bellnier**[b], and **Mukund Seshadri**[a,c,d,*]

[a]Department of Head and Neck Surgery, Roswell Park Cancer Institute, Elm and Carlton streets, Buffalo, NY, USA

[b]Department of Cell Stress Biology (Photodynamic Therapy Center), Roswell Park Cancer Institute, Elm and Carlton streets, Buffalo, NY, USA

[c]Department of Pharmacology and Therapeutics, Roswell Park Cancer Institute, Elm and Carlton streets, Buffalo, NY, USA

[d]Department of Dentistry and Maxillofacial Prosthetics, Roswell Park Cancer Institute, Elm and Carlton streets, Buffalo, NY, USA

Abstract

Objective—Photodynamic therapy (PDT) is a clinically approved minimally invasive treatment for cancer. In this preclinical study, using an imaging-guided approach, we examined the potential utility of PDT in the management of bulky squamous cell carcinomas (SCCs).

Methods—To mimic bulky oropharyngeal cancers seen in the clinical setting, intramuscular SCCs were established in six-to-eight week old female C3H mice. Animals were injected with the photosensitizer, 2-[hexyloxyethyl]-2-devinyl pyropheophorbide-a (HPPH; 0.4 μmol/kg, i.v.) and tumors were illuminated 24 hours post injection with 665 nm light. PDT as a single treatment modality was administered by surface illumination or by interstitial placement of fibers (iPDT). Magnetic resonance imaging was used to guide treatment and assess tumor response to PDT along with correlative histopathologic assessment.

Results—Interstitial HPPH-PDT resulted in a marked change on T2 maps 24 hours post treatment compared to untreated controls or transcutaneous illumination. Corresponding apparent diffusion coefficient maps also showed hyperintense areas in tumors following iPDT suggestive of effective photodynamic cell kill. Histologic sections (H&E) confirmed presence of extensive tumor necrosis following iPDT.

© 2013Asian Association of Oral and Maxillofacial Surgeons. Published by Elsevier Ltd. All rights reserved

[*]*Corresponding author*: Dr. Mukund Seshadri Roswell Park Cancer Institute Elm and Carlton streets, CGP L4-314, Buffalo, New York 14263 Mukund.Seshadri@roswellpark.org Ph: 716-845-1552 Fax: 716-845-8857.

Publisher's Disclaimer: This is a PDF file of an unedited manuscript that has been accepted for publication. As a service to our customers we are providing this early version of the manuscript. The manuscript will undergo copyediting, typesetting, and review of the resulting proof before it is published in its final citable form. Please note that during the production process errors may be discovered which could affect the content, and all legal disclaimers that apply to the journal pertain.

CONFLICT OF INTEREST: None

Author Manuscript Author Manuscript Author Manuscript Author Manuscript

Conclusions—These results highlight the potential utility of PDT in the treatment of bulky oropharyngeal cancers. The findings of our study also demonstrate the utility of MRI as a non-invasive tool for mapping of early tissue response to PDT.

Keywords

photodynamic therapy; image-guided interstitial PDT; head and neck squamous cell carcinoma; magnetic resonance imaging

INTRODUCTION

Squamous cell carcinomas (SCCs) of the tonsils and tongue base (oropharynx) are locally and regionally aggressive tumors that result in debilitating changes in appearance, speech, deglutition and respiratory function in patients [1]. Standard treatment approaches such as surgery and chemoradiation often result in prolonged and severe morbidities including xerostomia, trismus, dysphagia, loss of dentition and mandibular osteoradionecrosis [2-4]. Clearly, there is a need to investigate novel strategies that can be effective in treating the disease without associated long-term toxicities and treatment-related complications.

Photodynamic therapy (PDT) is a clinically approved treatment for cancer that involves localized activation of a drug (photosensitizer) using light of a specific wavelength (Figure 1A) which in turn results in cell kill and vascular damage within the tumor [5]. Clinically, PDT offers a minimally invasive alternative to traditional anticancer therapies (chemotherapy, radiation) without risk of permanent, systemic sequelae in patients [6]. Additionally, PDT may be repeated when necessary without risk of additional toxicities and is often associated with favorable cosmetic and functional outcomes [6-8]. The potential of PDT against head and neck cancers has been active area of investigation [9-12]. Retrospective analysis of outcomes in 170 patients with early stage oral cavity and oropharyngeal cancers have revealed overall response rates and complete response rates of 90% and 70% respectively [11]. We have recently demonstrated the safety of PDT against premalignant and early malignant lesions of the oral cavity and larynx with encouraging results on treatment efficacy [12].

The most common approach to PDT involves surface illumination of tumors (Figure 1B) following intravenous administration or topical application of a photosensitizer. This transcutaneous approach for tumor illumination is often effective in treating early stage lesions of the head and neck that are limited in depth. However, this manner of light delivery may only result in limited photoactivation within thicker (bulkier) solid tumors similar to those seen in the tongue base and the oropharynx. To address this issue, preclinical and clinical studies have investigated the potential of interstitial PDT (iPDT), in which light is delivered through optical fibers inserted into the solid tumor mass (Figure 1B) with encouraging results [13-15].

The overall objective of the present study was to characterize the response of SCCs to iPDT. To mimic bulky oropharyngeal cancers observed in the clinical setting, intramuscular tumors were established in mice. Magnetic resonance imaging (MRI) was utilized to guide placement of the fiber for iPDT. Multiparametric MR mapping (T2-weighted and diffusion

Author Manuscript Author Manuscript Author Manuscript Author Manuscript

weighted imaging) along with correlative histopathology was performed to compare the photodynamic tissue damage following surface illumination or interstitial delivery of light to tumors. The utility of PDT as an intraoperative adjuvant treatment was also studied.

MATERIALS AND METHODS

Cell culture

SCCVII cells (kindly provided by Dr. Candace Johnson, Roswell Park Cancer Institute) were grown in RPMI medium (purchased from the Tissue Culture Facility at Roswell Park Cancer Institute) supplemented with 10% fetal bovine serum and 1% penicillin at 37°C. The cell monolayer was washed with phosphate-buffered saline (pH 7.4), trypsinized using EDTA (ethylenediaminetetraacetic acid). Cells were counted in a hemocytometer using 0.4% tryptan blue and prepared at the required concentration for *in vivo* inoculation.

Animals and tumor model

Female C3H/HeRos mice were obtained from the Laboratory Animal Resource at Roswell Park Cancer Institute. Animals were housed in micro isolator cages within the resource and provided food and water *ad libitum*. For experimental studies, a cell suspension was prepared and 3.5×10^5 SCCVII cells (50μl injection volume) were injected intramuscularly (into the thigh muscle) of eight-to-twelve week old animals. All procedures were carried out in accordance with protocols approved by the Institutional Animal Care and Use Committee at Roswell Park Cancer Institute.

Photosensitizer

Clinical-grade, pryogen-free 2-[1-hexyloxyethyl]-2-devinyl pyropheophorbide-a (HPPH) [16, 17] was obtained from the Roswell Park Pharmacy and reconstituted in pyrogen-free 5% dextrose (D5W; Baxter Corp.) containing 2% ethanol and 0.1% Tween. Tumor-bearing mice were administered 0.4μmol/kg of HPPH by tail vein injection.

PDT Protocol

Localized illumination of tumors was carried out 24 hours after photosensitizer administration. The light source consisted of a dye laser (375; Spectra-Physics) pumped by an argon ion laser (Spectra-Physics). The dye laser, using 4-dicyanomethylene-2-methyl-6-*p*-dimethylaminostyryl-4Hpyran (DCM) dye (Exciton), was tuned to 665nm. For interstitial light treatment, a 23-gauge needle was used to pierce through the skin of the tumor and create a path for placement of the fiber. A cylindrical diffuser fiber (1 cm) was then inserted into a depth of 4-5 mm. To enable maximal tumor illumination, the fiber was placed in the central region of the tumor. A total light dose of 135 J/cm was delivered at an irradiance of 75 mW/cm. An integrating sphere was used to measure the output from the fiber. Surface illumination of tumors was also performed using flat-cut fibers positioned ~9 cm above the tumor which provided a 1 cm treatment field. A power meter was used to measure the output of the fiber prior to surface illumination of the tumors (light dose of 135 J/cm^2 at a fluence rate of 75 mW/cm^2; treatment time = 30 minutes). Control animals received the sensitizer but were not illuminated. Fiber-only controls were also included to account for any changes in MR contrast induced by interstitial placement of the fiber.

Author Manuscript Author Manuscript Author Manuscript Author Manuscript

Magnetic resonance imaging

MRI examinations were carried out in a 4.7 T/33-cm horizontal bore magnet (GE NMR Instruments, Fremont, CA) incorporating AVANCE digital electronics (Bruker Biospec with ParaVision 3.0.2; Bruker Medical Inc., Billerica, MA) and a removable gradient coil insert (G060, Bruker Medical Inc., Billerica, MA) generating maximum field strength of 950 mT/m and a custom-designed 35-mm RF transmit-receive coil. Mice were placed on a form-fitted MR-compatible sled (Dazai Research Instruments, Toronto, Canada) and supplied with 2% isoflurane during image acquisition. Respiration rates and core-body temperature were monitored continuously while mice were in the scanner. Sagittal and coronal scout scans were run to localize tumors in mice and for slice prescription of subsequent scans. Coronal T2W images were acquired at different times post implantation to assess tumor growth (TE_{eff} = 41ms, TR = 2500ms, FOV = 4.8 × 3.2cm, RARE/echoes = 8/8, NEX = 4, matrix size = 256 x 192, 21 slices, slice thickness 1mm). T2-relaxation rate measurements were performed using a multi-echo CPMG spin echo sequence (TR = 2793ms, TE = 15-300ms, FOV = 3.2 × 3.2 cm, matrix size = 192×192, 5 slices, slice thickness 1mm, number of echoes = 20). Diffusion-weighted imaging (DWI) was performed using a muti-slice diffusion-weighted spin echo sequence with the following parameters: TE/TR = 30/1200ms, matrix size = 128× 128, FOV 3.2 × 3.2 cm, NEX = 2, diffusion gradient strength (four variable gradient strengths per acquisition) = 8, 128, 256, 420mT/M, diffusion B value = 2.9, 512, 2036, 5470 s/mm^2, diffusion gradient duration = 6ms, diffusion gradients applied in the X, Y, and Z directions, slice thickness – 1mm, 5 slices [18]. Three-dimensional spoiled gradient echo scans were acquired using the following parameters: FOV 4.8 × 3.2 × 3.2, matrix size 192 × 128 × 128, TR = 15 ms, TE_{eff} = 3.0 ms, NEX = 2, slice thickness = 32 mm, flip angle = 40°, acquisition time = 8m11s.

Image processing and analysis

Commercially available medical imaging software (Analyze; Version 7.0; Overland Park, KS) was used to process the raw image data sets. T2 maps and apparent diffusion coefficient (ADC) maps were generated on a pixel-by-pixel bases in MATLAB (Version 7.0, Mathworks Inc., Natick, MA) and pseudo-colorized for visualization using Analyze (AnalyzeDirect, Overland Park, KS). Object maps were created by manually defining tumor, muscle tissue, phantom and background noise on T2W images. These object maps were then overlaid on T2 maps and ADC maps to determine T2 relaxation times and ADC values, respectively.

Histologic and immunohistochemistry

Tumors were excised following completion of imaging for immunohistochemical and histologic analysis. Immunostaining of tumor sections for the endothelial cell marker CD31 was performed as previously described [19]. Slides were counter stained with Harris hematoxylin (Poly Scientific, Bay Shore, NY). Glass slides containing tissue sections were scanned and digitized using the ScanScope XT system (Aperio Technologies, Vista, CA) and captured using ImageScope software (Aperio Technologies, Version 9.1; Vista, CA). The number of CD31+ vessels were counted in multiple fields (20X magnification, 5 fields

Author Manuscript Author Manuscript Author Manuscript Author Manuscript

per tumor) in control and PDT-treated tumors (n = 3-5 tumors per group) and reported as average microvessel density (MVD).

Statistical considerations

Statistical analysis was performed using GraphPad Prism Versions 5.00 for Windows (GraphPad Software, San Diego, CA). Data were tested for statistical significance using an unpaired two-tailed student's *t* test analysis. Median survival was calculated from Kaplan-Meier survival curves and differences were analyzed by the log-rank test. Values are reported as mean ± standard error of the mean.

RESULTS

The study design and timeline are shown schematically in Figure 1. Initial MRI examinations were performed ~5-7 days post implantation to confirm tumor establishment and to assess morphology of the intramuscular tumors. Multislice T2-weighted images revealed successful growth of SCC tumors in the thigh muscle of mice. Figure 2A shows coronal T2-weighted images of a mouse bearing bilateral intramuscular SCCVII tumors (*outlined in yellow*) on day 5 and day 10 post-implantation. Tumors appeared relatively homogenous with minimal areas of hemorrhaging (hypointense regions) or necrosis (hyperintense regions). Coronal T2-weighted images and three-dimensional images were acquired following interstitial placement of the fiber into the tumor (n = 3). Figure 2B shows contiguous slices from a 3D scan with the fiber trace visible within the tumor (*denoted by the arrow*).

Following confirmation of tumor growth *in vivo*, tumor-bearing animals were randomized into either the drug only control arm, iPDT arm or transcutaneous PDT arm. Mean tumor volumes of animals in the iPDT (564 ± 98 mm^3; n = 4) and transcutaneous PDT (546 ± 73 mm^3; n = 3) were comparable to control tumors (538 ± 31 mm^3; n= 6). T2 mapping was performed at baseline and 24 hours post PDT. To account for any changes in T2 contrast induced by the presence of the optical fiber in the tumor interstitium, true controls (fiber-only) were also utilized. For these fiber-only controls, interstitial fibers were placed into the tumors of animals that did not receive any photosensitizer for the duration of light treatment (approximately 30 mins) and T2 mapping was performed 24 hours fiber insertion. The top panel of images shown in Figure 3 represents pseudo-colorized T2-maps of SCCVII tumors from fiber only control and iPDT groups. SCCVII tumors treated with iPDT showed a marked change in T2 relaxation time compared to fiber only control tumors. Average T2 values of untreated control SCCVII tumors, tumors treated with surface illumination, and tumors treated with ID-PDT were also calculated. Placement of fiber alone did not result in any significant change ($p>0.1$) in T2 values (71 ± 0.6 ms; n = 3) compared to untreated drug only controls (74 ± 1.3 ms; n = 6). Mean T2 values of tumors treated with iPDT (84 ± 3.0 ms; n = 4) were significantly higher ($p<0.01$) than controls suggestive of increased photodynamic damage (vascular occlusion/necrosis). Diffusion-weighted imaging [20] was also carried out to assess changes in cellularity following treatment. A spatially heterogeneous ADC response was observed 24 hours after iPDT. Regions with higher T2 values also exhibited higher ADC (Figure 3, *lower panel*, *arrows*) suggestive of PDT-

Author Manuscript Author Manuscript Author Manuscript Author Manuscript

induced tumor necrosis. ADC values (1×10^{-3} mm^2/sec) of tumors treated with iPDT (0.64 ± 0.04; n = 4) were significantly higher ($p<0.05$) than control tumors (0.50 ± 0.03, n = 6). In comparison, T2 maps of tumors treated with transcutaneous illumination showed minimal changes within the tumor 24 hours post illumination (Figure 4). Mean T2 values of tumors treated with transcutaneous PDT (77 ± 2.0 ms) did not show a significant change ($p>0.05$) compared to controls. Quantitative estimates of ADC did not reveal a significant ($p>0.05$) difference between control and transcutaneous-PDT (0.57 ± 0.01; n = 3) groups. No significant difference in contrast was observed between ADC maps of drug only or fiber only control tumors.

Consistent with the imaging results results, H&E sections of tumors excised 24 hours post iPDT (Figure 5, *bottom*) showed marked necrosis with increased intercellular space and pyknotic nuclei. Untreated control SCCVII tumor shows dense, viable appearing tumor cells (Figure 5, *top*). Tumors treated with transcutaneous PDT showed regional changes on ADC maps and minimal evidence of necrosis on histologic sections (Figure 5, *middle*). CD31-immunostaining of tumor sections was also performed to assess vascular damage following iPDT. As shown in Figure 6, control tumors appeared well vascularized with distinct clusters of CD31+ vessels visible under high power (20 X magnification). In contrast, tumors treated with iPDT showed evidence of vascular damage and a reduction in microvessel density (MVD) count compared to controls ($p<0.05$) and tumors treated with transcutaneous PDT ($p<0.01$). MVD analysis did not reveal any difference between control tumors and tumors treated with transcutaneous PDT.

DISCUSSION

Photodynamic therapy (PDT) is a clinically approved treatment for cancer that involves localized activation of a drug (photosensitizer) using light of a specific wavelength which in turn results in cell kill and vascular damage within the tumor. Preclinical and clinical trials have shown PDT to be promising for the treatment of head and neck cancers [9-12, 21]. However, photodynamic treatment of bulky invasive oropharyngeal cancers is likely to require interstitial placement of multiple laser fibers into the tumor tissue to enable uniform and adequate illumination of all the regions within the tumor. The overall objective of this preclinical study was to characterize the response of bulky invasive SCCs to iPDT. Since oropharyngeal cancers, particularly tongue base cancers are often locally aggressive and tend to involve extrinsic (deep) muscles of the tongue, we utilized an intramuscular model of SCC to examine the potential of iPDT. Our results demonstrate the potential role of PDT in the management of head and neck cancer. Specifically, our results suggest that interstitial PDT (rather than surface illumination) is likely to exhibit improved therapeutic efficacy against bulky, deep-seated head and neck tumors. Our findings also highlight the potential utility of MRI in the guidance of fiber placement and assessment of acute changes following iPDT *in vivo*.

The ability to obtain an early read-out of tumor response would be valuable in the clinical development of PDT. In this regard, the use of non-invasive imaging methods including MRI and ultrasound has been previously explored [22, 23]. We utilized MRI to guide interstitial placement and assess tumor response to iPDT using the photosensitizer HPPH.

Author Manuscript Author Manuscript Author Manuscript Author Manuscript

MRI methods that have been employed to assess tumor response to PDT include T1-weighted contrast-enhanced MRI [15], T2W-MRI [24, 25] and DWI [26]. However, a majority of preclinical studies investigating MRI methods have typically utilized the response of subcutaneous tumors to surface illumination. We have previously utilized T1-weighted contrast-enhanced MRI and T2-weighted MRI to characterize the vascular response to PDT in preclinical models [24, 27]. In the present study, we utilized combined T2 mapping and DWI for non-invasive monitoring of tissue response to iPDT. The T2 - relaxation time (transverse relaxation) of water protons is affected by changes in molecular, physical and chemical environment within tissue [28]. PDT causes vascular damage, cell necrosis, and an inflammatory response, all of which would influence the water content and distribution within the tumor, accounting for the observed changes in T2 contrast. As early as 24 hours after iPDT, T2 mapping revealed marked changes in contrast within tumors. Mean T2 values of iPDT treated tumors were higher compared to control tumors and tumors treated with transcutaneous PDT. These findings are consistent with another study that showed an increase in T2 values after PDT in a prostate tumor model [25]. Changes in T2-contrast were much more pronounced with iPDT compared to transcutaneous illumination of tumors, suggestive of increased photodynamic efficacy. One possible explanation for this observation is limited or insufficient delivery of light through the skin to deeper regions of the tumor preventing adequate photoactivation of the sensitizer within the tumor. The depth of light penetration is dependent on wavelength of light and tissue optical properties. In our study, we utilized the photosensitizing agent HPPH which is activated at 665nm. Light at this wavelength penetrates to a depth of 3mm from the dorsal surface of the human tongue (Bellnier, unpublished observation). Although insertion of the optical fiber could lead to inflammatory changes within the tumor and alterations in T2 contrast, T2 values of untreated controls vs. fiber only control tumors were comparable ($p>0.05$), validating that these observed changes in T2 contrast were treatment-related. Immunohistochemical and histologic analysis of the SCCVII tumors confirmed vascular damage and tumor necrosis following iPDT.

We utilized DWI to assess tumor cell kill following iPDT. ADC maps provide an estimate of the mobility of water molecules in tissue [20]. ADC maps, calculated from DWI, showed areas of hyperintensity in SCCVII tumors 24 hours after iPDT, which suggests tumor necrosis. Tumor cell death following PDT would result in increased water diffusion through the release of intracellular water, which would account for the hyperintensity seen on ADC maps 24 hours after iPDT. Measured values of ADC were higher in iPDT treated tumors compared to transcutaneous illumination or untreated controls. Diffusion-weighted imaging has been previously utilized to assess response to PDT [15, 26]. Wang and Fei have demonstrated an increase in ADC 24 hours after PDT in tumors following transcutaneous illumination [27]. In the study by Huang et al [15], alterations in contrast were noted following PDT on DWI but ADC mapping did not consistently delineate necrotic areas. It could be speculated that the heterogeneity in the ADC response could be related to the complex biological response to PDT that includes the onset of necrosis and edema along with vascular occlusion and hemorrhaging. These competing changes occurring within the tumor microenvironment could explain the lack of robust changes in contrast with DWI. Given the temporal nature of tissue response to PDT, the authors suggest that acquisition of

Author Manuscript Author Manuscript Author Manuscript Author Manuscript

DWI datasets at later time points (few days post therapy) would perhaps eliminate some of these confounding biological changes and provide a clear read-out of PDT-induced cell kill on DWI.

We recognize the limitations of our study. Dosimetry in PDT is critical and complex especially with interstitial light delivery [29]. We did not perform dosimetric analysis to assess the extent of light distribution in these bulky tumors following our iPDT protocol. While we used the same total light dose and treatment time for both the surface illumination and iPDT groups, the actual tumor doses may not be comparable due to the physical properties of light distribution. Ongoing studies by our group are aimed at mathematical modeling of light dosimetry *in vivo* using real-time measurement of tissue optical properties. Once developed, we intend to integrate optical dosimetry into treatment planning for subsequent clinical trials of iPDT.

In conclusion, the results of our study demonstrate the potential of MRI-guided interstitial PDT for the management of bulky head and neck cancers. In a recent study by Jerjes *et al*, ultrasound-guided iPDT of stage IV tongue base carcinoma patients was performed using the sensitizer, mTHPC [23]. Taken together, these results demonstrate the feasibility of imaging-guided PDT in the clinical setting for treatment of deep seated tumors. The excellent soft tissue contrast of MRI along with its functional capabilities could make it an effective clinical tool to guide fiber placement and assess early treatment response to iPDT.

ACKNOWLEDGEMENTS

This work was supported by grants from the National Cancer Institute (PO1CA055791) and the Roswell Park Alliance Foundation (M.S., and D.B.) and utilized core resources supported by RPCI's Cancer Center Support Grant from the NCI P30CA16056 (Trump, DL). The sponsor did not have any involvement in the design and conduct of the research. The authors would like to acknowledge Patricia Manderscheid and Steve Turowski for valuable technical assistance and Dr. Mihai Merzianu for assistance in histopathologic analysis.

REFERENCES

1. Marur S, Forastiere AA. Head and neck cancer: changing epidemiology diagnosis and treatment. Mayo Clin Proc. 2008; 83:604.
2. Jones AS, Rafferty M, Fenton JE, Jones TM, Husband DJ. Treatment of squamous cell carcinoma of the tongue base: irradiation, surgery or palliation? Ann Otol Rhinol Laryngol. 2007; 116:92–99.
3. Cano ER, Lai SY, Caylakli F, Johnson JT, Ferris RL, Carrau RL, et al. Management of squamous cell carcinoma of the base of tongue with chemoradiation and brachytherapy. Head Neck. 2009; 31:1431–38. [PubMed: 19405086]
4. O'Neill JP, Hughes JP, Manning KP, Fenton JE. Controversies in the management of tongue base cancer. Ir J Med Sci. 2009; 178:1–5. [PubMed: 18810572]
5. Dougherty TJ, Gomer CJ, Henderson BW, Jori G, Kessel D, Korbelik M, et al. Photodynamic therapy. J Natl Cancer Inst. 1998; 90:889–905. [PubMed: 9637138]
6. Hopper C. Photodynamic therapy: A clinical reality in the treatment of cancer. Lancet Oncol. 2000; 1:212–19. [PubMed: 11905638]
7. Nyst HJ, Tan IB, Stewart FA, Balm AJ. Is photodynamic therapy a good alternative to surgery and radiotherapy in the treatment of head and neck cancer? Photodiagnosis Photodyn Ther. 2009; 6:3–11. Review. [PubMed: 19447366]
8. Lou PJ, Jones L, Hopper C. Clinical outcomes of photodynamic therapy for head-and-neck cancer. Technol Cancer Res Treat. 2003; 2:311–7. [PubMed: 12892513]

Author Manuscript Author Manuscript Author Manuscript Author Manuscript

9. Biel MA. Photodynamic therapy and the treatment of head and neck neoplasia. Laryngoscope. 1998; 108:1259–68. [PubMed: 9738739]
10. Biel MA. Photodynamic therapy treatment of early oral and laryngeal cancers. Photochem Photobiol. 2007; 83:1063–68. [PubMed: 17880501]
11. Karakullukcu B, Oudenaarde Kv, Copper MP, Klop WMC, van Veen R, Wildeman M, et al. Photodynamic therapy of early stage oral cavity and oropharynx neoplasms: an outcome analysis of 170 patients. Eur Arch Otorhinolaryngol. 2011; 268:281–8. [PubMed: 20706842]
12. Rigual NR, Thankappan K, Cooper M, Sullivan MA, Dougherty TJ, Popat SR, et al. Photodynamic Therapy for Head and Neck Dysplasia and Cancer. Arch Otolaryngol Head Neck Surg. 2009; 135:784–88. [PubMed: 19687399]
13. Vogl TJ, Eichler K, Mack MG, et al. Interstitial photodynamic laser therapy in interventional oncology. Eur Radiol. 2004; 14:1063. [PubMed: 15045520]
14. Beck TJ, Kreth FW, Beyer W, Mehrkens JH, Obermeier A, Stepp H, et al. Interstitial photodynamic therapy of nonresectable malignant glioma recurrences using 5-aminolevulinic acid induced protoporphyrin IX. Lasers Surg Med. 2007; 39:386–93. [PubMed: 17565715]
15. Huang Z, Haider MA, Kraft S, Chen Q, Blanc D, Wilson BC, et al. Magnetic resonance imaging correlated with the histopathological effect of Pdbacteriopheophorbide (Tookad) photodynamic therapy on the normal canine prostate gland. Lasers Surg Med. 2006; 38:672–81. [PubMed: 16799982]
16. Henderson BW, Bellnier DA, Greco WR, Sharma A, Pandey RK, Vaughan LA, et al. An in vivo quantitative structure-activity relationship for a coneneric series of pyropheophorbide derivatives as photosensitizers fo photodynamic therapy. Cancer Res. 1997; 57:4000–7. [PubMed: 9307285]
17. Bellnier DA, Greco WR, Nava H, Loewen GM, Oseroff AR, Dougherty TJ. Mild skin photosensitivity in cancer patients following injection of Photochlor (2-[1-hexyloxyethyl]-2-devinyl pyropheophorbide-a; HPPH) for photodynamic therapy. Cancer Chemother Pharmacol. 2006; 57:40–5. [PubMed: 16001178]
18. Seshadri M, Ciesielski MJ. MRI-based characterization of vascular disruption by 5,6-dimethylxanthenone-acetic acid in gliomas. J Cereb Blood Flow Metab. 2009; 29:1373–82. [PubMed: 19458603]
19. Seshadri M, Toth K. Acute vascular disruption by 5,6-dimethylxanthenone-4-acetic acid in an orthotopic model of human head and neck cancer. Transl Onc. Aug 18. 2009; 2(3):121–7.
20. Koh D, Collins D. Diffusion-weighted MRI in the body: applications and challenges in oncology. AJR. 2007; 188:1622–35. [PubMed: 17515386]
21. Jerjes W, Upile T, Radhi H, Hopper C. Photodynamic therapy and end-stage tongue base cancer: short communication. Head Neck Oncol. Dec 7.2011 3:49. [PubMed: 22152039]
22. Jäger HR, Taylor MN, Theodossy T, Hopper C. MR imaging-guided interstitial photodynamic laser therapy for advanced head and neck tumors. AJNR Am J Neuroradiol. 2005; 26:1193–200. [PubMed: 15891183]
23. Jerjes W, Upile T, Hamdoon Z, Abbas S, Akram S, Mosse CA, et al. Photodynamic therapy: The minimally invasive surgical intervention for advanced and/or recurrent tongue base carcinoma. Lasers Surg Med. 2011; 43:283–92. [PubMed: 21500222]
24. Seshadri M, Bellnier DA, Vaughan LA, Spernyak JA, Mazurchuk R, Foster TH, et al. Light delivery over extended time periods enhances the effectiveness of photodynamic therapy. Clin Cancer Res. 2008; 14:2796–805. [PubMed: 18451247]
25. Fei B, Want H, Meyers J, Feyes D, Oleinick N, Duerk J. High-field magnetic resonance imaging of the response of human prostate cancer to Pc 4-based photodynamic therapy in an animal model. Lasers in Surgery and Medicine. 2007; 39:723–30. [PubMed: 17960753]
26. Wang H, Fei B. Diffusion-weighted MRI for monitoring tumor response to photodynamic therapy. J Magn Reson Imaging. 2010; 32:409–17. [PubMed: 20677270]
27. Seshadri M, Spernyak JA, Mazurchuk R, Camacho SH, Oseroff AR, Cheney RT, et al. Tumor vascular response to photodynamic therapy and the antivascular agent 5,6-dimethylxanthenone-4-acetic acid: implications for combination therapy. Clin Cancer Res. 2005; 11:4241–50. [PubMed: 15930363]

Author Manuscript Author Manuscript Author Manuscript Author Manuscript

28. Lee SC, Poptani H, Pickup S, Jenkins WT, Kim S, Koch CJ, et al. Early detection of radiation therapy response in non-Hodgkin's lymphoma xenografts by in vivo 1H magnetic resonance spectroscopy and imaging. NMR Biomed. 2010; 23:624–32. [PubMed: 20661875]

29. Davidson SR, Weersink RA, Haider MA, Gertner MR, Bogaards A, Giewercer D, et al. Treatment planning and dose analysis for interstitial photodynamic therapy of prostate cancer. Phys Med Biol. 2009; 54:2293–313. [PubMed: 19305043]

Author Manuscript Author Manuscript Author Manuscript Author Manuscript

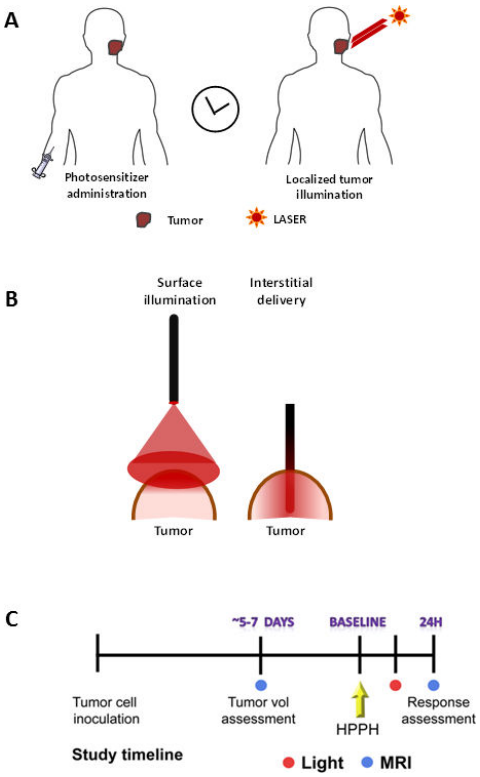

Figure 1.

(A) Basic methodology of PDT: PDT involves localized activation of a systemically administered photosensitizer by light of a specific wavelength from a laser light source**. (B)** Light delivery in PDT is typically performed by surface illumination of tumors using optical fibers or by interstitial delivery that involves placement of optical fibers into the tumor interstitium. **(C)** Schematic of experimental study design. Following inoculation of SCCVII tumor cells, animals underwent MRI examinations 5-7 days post injection to visualize tumor growth. Upon successful establishment of tumor growth (day 8-10), animals were randomized into control or PDT treatment arms. MRI and histologic response assessment was performed 24 hours post PDT.

Author Manuscript Author Manuscript Author Manuscript Author Manuscript

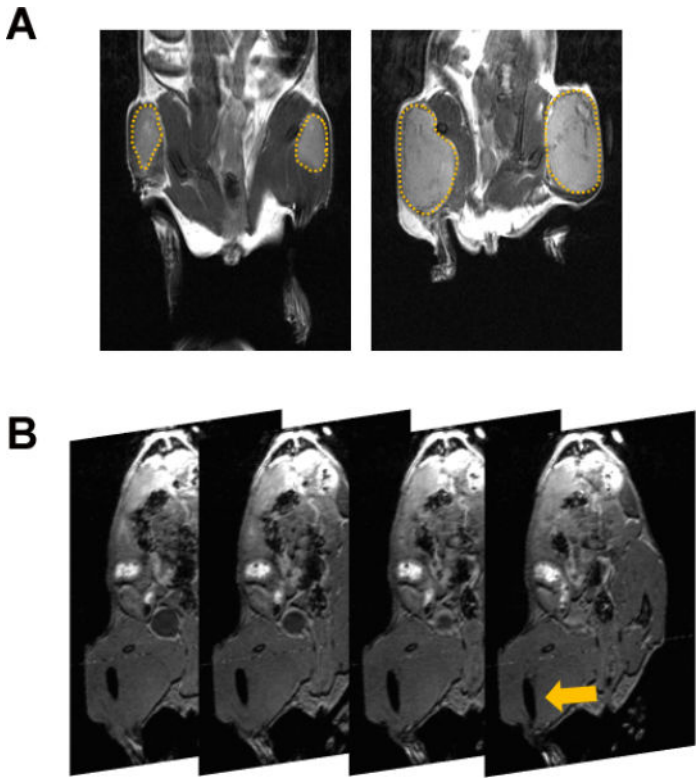

Figure 2. Image-guided interstitial PDT of SCC tumors

(A) Coronal T2-weighted MRI was performed at different times (days 5-10) post implantation for serial monitoring of the growth of intramuscular SCCVII tumors (*outlined in yellow*). **(B)** Contiguous slices from a 3D spoiled-gradient echo scan of a mouse bearing intramuscular SCCVII tumor with the visible trace of the fiber placed in the tumor interstitium (*arrow*).

Author Manuscript Author Manuscript Author Manuscript Author Manuscript

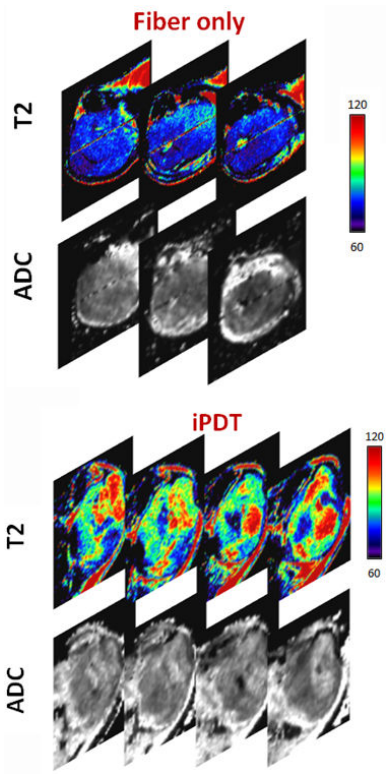

Figure 3. SCC response to interstitial-HPPH sensitized PDT

Panel of images represent calculated T2- maps (5 contiguous slices) of tumors in control and treatment groups. SCCVII tumors treated with interstitial PDT showed a marked change on T2 relaxation time compared to control tumors suggestive of increased photodynamic damage (vascular occlusion/necrosis). Placement of the optical fiber alone did not result in any visual change in T2 contrast. Tumors treated with transcutaneous PDT showed minimal change. Corresponding ADC maps (lower panel) also showed hyperintense regions within the tumors treated with interstitial PDT which is indicative of PDT-induced tumor cell kill.

Author Manuscript Author Manuscript Author Manuscript Author Manuscript

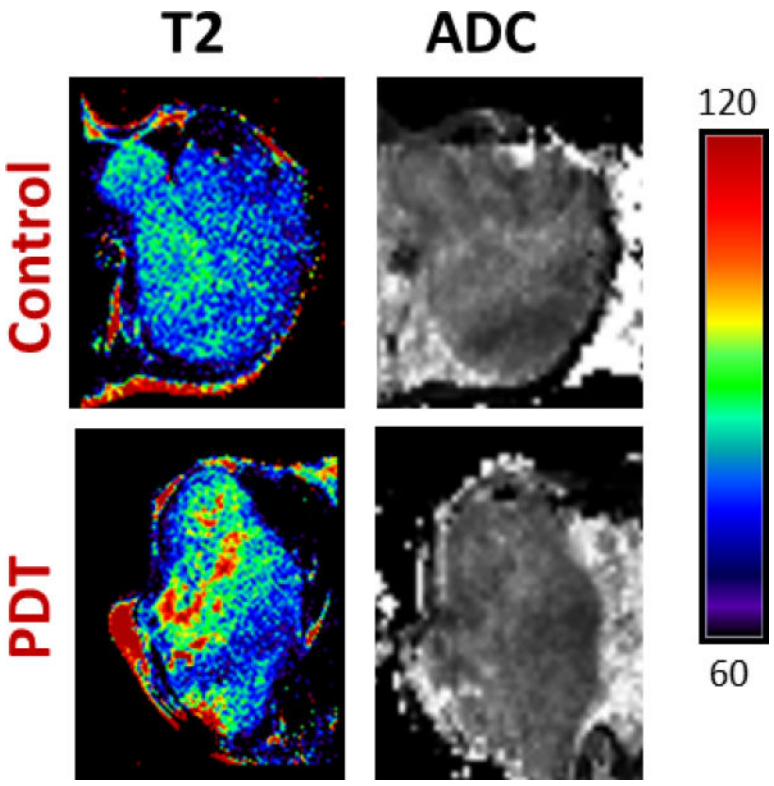

Figure 4. MR mapping of SCCVII response to PDT (transcutaneous illumination)

Panel of images represent T2 and ADC maps of a control SCCVII tumor and a tumor-treated with transcutaneous PDT. T2 mapping revealed minimal changes within the tumor following transcutaneous illumination at 24 hours post treatment. No visual evidence of photodynamic damage was seen on ADC maps following transcutaneous PDT compared to untreated control tumors.

Author Manuscript Author Manuscript Author Manuscript Author Manuscript

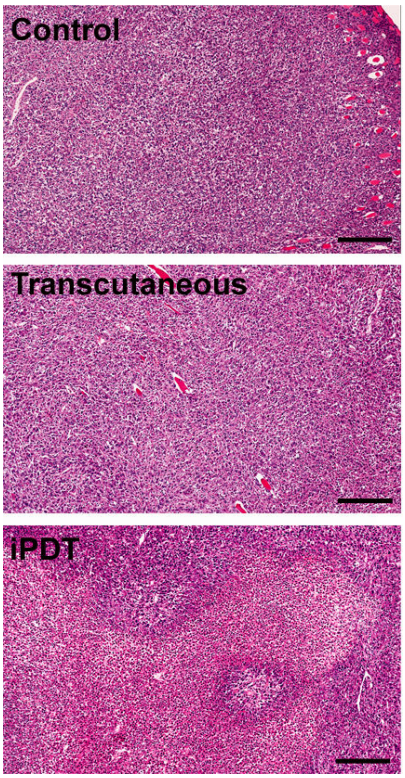

Figure 5. Histopathologic assessment of tumor response to iPDT

Panel of images represent hematoxylin and eosin (H&E; 10x magnification) sections of whole tumors excised 24 hours Untreated control SCCVII tumor sections shows tumor cells without necrosis. Tumors treated with iPDT showed increased areas of necrosis with increased intercellular space and pyknotic nuclei. In comparison, tumors treated with transcutaneous PDT showed minimal evidence of necrosis on histologic sections.

Author Manuscript Author Manuscript Author Manuscript Author Manuscript

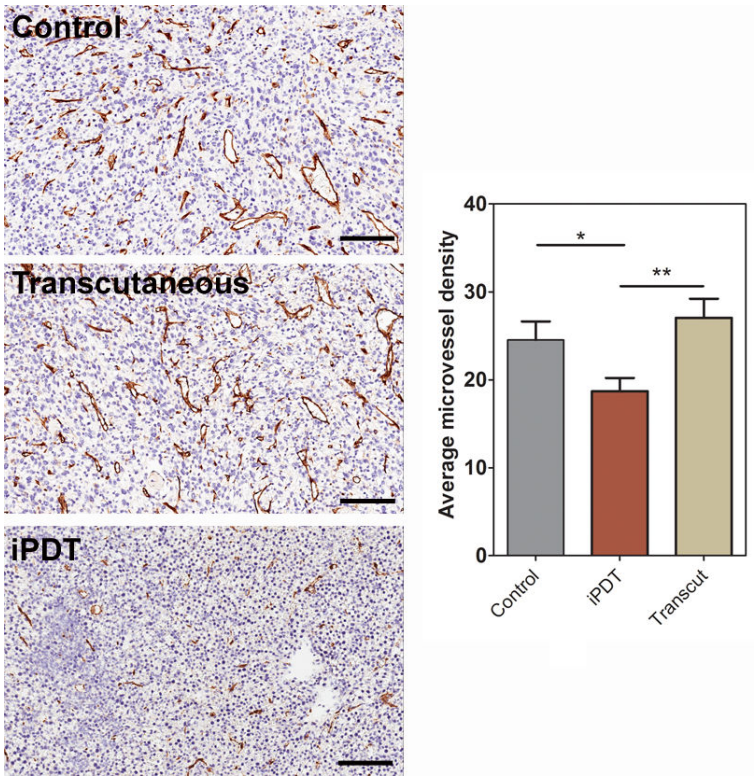

Figure 6. Immunohistochemical assessment of vascular response to iPDT

(A) Panel of images represent photomicrographs of CD31-immunostained tumor sections (20X magnification) from control and PDT-treated animals. (B) Microvessel density counts of control and PDT-treated tumors. CD31+ positive vessels were counted in multiple high power fields (5 fields per tumor, n=3-5 tumors per group) and reported as average microvessel density *$p<0.05$; **$p<0.01$.